Journal of Chromatography, 101 (1974) 1–16

CHROM. 7630

RADIAL TEMPERATURE DISTRIBUTION IN ISOTACHOPHORESIS COLUMNS OF CIRCULAR CROSS-SECTION

M. COXON and M. J. BINDER

Aerospace and Mechanical Engineering Department, University of Arizona, Tucson, Ariz. 85721 (U.S.A.)

(Received May 15th, 1974)

SUMMARY

An analysis of the unsteady-state heat-conduction problem in isotachophoretic columns of circular cross-section is given, based on a linear variation of electrical conductivity with temperature and taking into account the effects of a finite wall thickness. It is seen that previous analyses, based on constant electrical conductivity, tend to underpredict actual temperature distributions considerably. The use of thick-walled columns is seen to be advantageous both from the viewpoint of higher resolution and of increased production.

INTRODUCTION

Joule heating, caused by the passage of current through an electrophoresis column, produces radial temperature gradients in which the temperature is highest at the axis of the column and declines toward the periphery. A precise determination of radial temperature distributions is essential for two very important reasons. First, because ionic mobilities are temperature dependent (increasing about 2%/°K), a radial temperature distribution produces variations in migration velocity across the tube, thus causing "bowing" of the frontal (ionic species interface) regions. Secondly, in the case of living cells relatively small temperature changes can be tolerated over the cross-section of the column if cell damage is to be avoided (0 to 37°C when using an aqueous solvent). This requires the solution to the transient heat-conduction problem as the system must be designed in such a way that the time required for separation is less than the time required for the system to reach this critical temperature at which cell destruction begins.

We consider the isotachophoresis to occur in a glass-walled column of circular cross-section. The voltage drop along the tube is assumed to be independent of the temperature and hence of the radial location. It follows that the current density is then a function of radial location because of the temperature dependence of the electrical conductivity.

The present solution is based on the following assumptions.

(1) Convective effects may be ignored;

(2) The fluid supporting medium is essentially at rest with the various ionic species drifting through it in the axial direction;

(3) The thermal properties (density, specific heat and thermal conductivity) are independent of temperature;

(4) The electrical conductivity is a linear function of the temperature over the range of temperatures of interest;

(5) The temperature distribution may be obtained as the solution of a conduction problem involving only the radial coordinate and time.

Some further comments are in order with respect to these assumptions.

Assumption 5 will be a good approximation in any longitudinal (axial) region sufficiently far away from any fronts where it is obvious that strong longitudinal temperature gradients must exist. It may be argued that it is precisely in the region of the fronts that we wish to determine the effects of non-uniformities in the temperature distribution. However, the present approach is a legitimate first step towards the more general problem and certainly should permit a first-order estimate of the temperature dependence of the species migration-velocity profile to be determined. Furthermore, it is clear that there is always one region (the terminator) where the heat generation is a maximum and this region is not a sample region. Thus, if the maximum design temperature is specified in this region, there will be no danger of the sample species becoming overheated. Present calculations permit the determination of the time taken to reach maximum design temperature and the corresponding maximum electric field strength.

Assumption 1 will certainly be valid in gels, and because we are considering applications for manufacturing in space where operation will occur in a gravity-free environment, it should also be valid in free solution provided electroconvective effects may be neglected. Preliminary investigations in Skylab indicate that this may not be a major factor.

In view of assumption 2 the present results will not apply to any system using a free solution with counterflow.

Assumption 3 has been checked by comparing the "exact" steady-state constant-properties solution with the results of a steady-state perturbation analysis which permits variation in the thermal properties with temperature. It appears that the effect of neglecting thermal-property variations is very small and that the results of a constant-property analysis are conservative. Details of this particular point are discussed in the Appendix.

PREVIOUS WORK

Martin and Everaerts[1] have considered a steady-state analysis under the assumptions of constant thermal and electrical conductivity and specific heat. They obtain an expression for the difference between the temperature at the center of the column and that at any radius r. This temperature distribution is parabolic and neglects the effects of column wall thickness. Assuming a mobility increase with temperature of 2%/°K, they obtain an expression for the variation of mobility due to this radial temperature distribution.

Konstantinov and Oshurkova[2], using the same assumptions as above, obtain a similar expression for the difference in temperature between a point at radius r

and the inside column wall. Using the 2%/°K mobility variation with temperature they arrive at an expression for the velocity variation across the column.

Hjertén[3], considering free zone electrophoresis, makes the same assumptions as in the above two cases, and also imposes the condition that the temperature variation across the column be much smaller than the cooling-bath temperature and thus obtains a parabolic velocity profile. He states that the migration-velocity profile in a temperature gradient is determined almost entirely by the temperature variation of viscosity, and suggests the use of a counterflow of buffer to flatten curved zones.

Routs[4], basing his observations on the work of Hjertén, notes that, because electrical conductivity decreases from the leading electrolyte to the terminator, the boundaries of the zones near the terminator will be more curved than the boundaries of the high-conductivity zones. He further states that the only way to straighten the fronts is to reduce the field strength because the use of counterflow to restore the boundaries of the terminating zones includes the danger of destroying the straighter fronts of the leading ion zones.

Brown and Hinckley[5] consider a linear variation of electrical conductivity with temperature and include the effects of the presence of a finite wall thickness and thus obtain expressions for the temperature profiles in the electrolyte solution and in the column wall for the steady-state condition, based on a constant-temperature boundary condition on the outside wall.

STATEMENT OF THE PROBLEM

Mathematically the problem may be stated as follows:

$$K_1 \left\{\frac{1}{r}\frac{\partial}{\partial r}\left(r\frac{\partial T_1}{\partial r}\right)\right\} = \frac{\partial T_1}{\partial t} - \frac{Q_e}{\varrho_1 c_1}, \quad 0 \leqslant r \leqslant R_1$$

$$K_2 \left\{\frac{1}{r}\frac{\partial}{\partial r}\left(r\frac{\partial T_2}{\partial r}\right)\right\} = \frac{\partial T_2}{\partial t}, \quad R_1 \leqslant r \leqslant R_2$$

$$T_1 = T_2 \text{ at } r = R_1,\ t > 0$$

$$k_1\frac{\partial T_1}{\partial r} = k_2\frac{\partial T_2}{\partial r} \text{ at } r = R_1,\ t > 0$$

T_1 finite at $r = 0$.

$$k_2\frac{\partial T_2}{\partial r} + h(T_2 - T_\infty) = 0 \text{ at } r = R_2,\ t > 0$$

$$T_1 = T_\infty \text{ in } 0 \leqslant r \leqslant R_1,\ t = 0$$

$$T_2 = T_\infty \text{ in } R_1 \leqslant r \leqslant R_2,\ t = 0.$$

We introduce the dimensionless variables

$$\theta = \frac{T - T_\infty}{T_\infty},\ \xi = \frac{r}{R_2},\ \tau = \frac{K_1 t}{R_2^2}$$

and assume that

$$Q_e = Q_0 (1 + \alpha\theta) = JE^2\sigma = JE^2\sigma_0 (1 + \alpha\theta)$$

where the heat generation per unit volume and the electrical conductivity are denoted by Q_0 and σ_0, respectively, when evaluated at $\theta = 0$.

We also denote

$$S = \frac{Q_0 R_2^2}{k_1 T_\infty}$$

$$\gamma = \frac{h R_2}{k_2}$$

$$\xi_1 = R_1/R_2$$

Then the statement of the problem in dimensionless variables is:

$$\frac{1}{\xi}\frac{\partial}{\partial\xi}\left(\xi\frac{\partial\theta_1}{\partial\xi}\right) = \frac{\partial\theta_1}{\partial\tau} - S(1 + \alpha\theta_1), \quad 0 \leqslant \xi \leqslant \xi_1$$

$$\frac{1}{\xi}\frac{\partial}{\partial\xi}\left(\xi\frac{\partial\theta_2}{\partial\xi}\right) = \frac{K_1}{K_2}\frac{\partial\theta_2}{\partial\tau}, \quad \xi_1 \leqslant \xi \leqslant 1$$

$$\theta_1 = \theta_2 \text{ at } \xi = \xi_1$$

$$k_1\frac{\partial\theta_1}{\partial\xi} = k_2\frac{\partial\theta_2}{\partial\xi} \text{ at } \xi = \xi_1$$

$$\theta_1 \text{ finite at } \xi = 0$$

$$\frac{\partial\theta_2}{\partial\xi} + \gamma\theta_2 = 0 \text{ at } \xi = 1$$

$$\theta_1 = 0 \text{ in } 0 \leqslant \xi \leqslant \xi_1, \tau = 0$$

$$\theta_2 = 0 \text{ in } \xi_1 \leqslant \xi \leqslant 1, \tau = 0$$

This problem is split into steady-state and transient parts by writing

$$\theta(\xi,\tau) = \theta^s(\xi) + \theta^t(\xi,\tau)$$

Steady-state problem

$$\frac{1}{\xi}\frac{\mathrm{d}}{\mathrm{d}\xi}\left(\xi\frac{\mathrm{d}\theta_1^s}{\mathrm{d}\xi}\right) = -S(1 + \alpha\theta_1^s), \quad 0 \leqslant \xi \leqslant \xi_1$$

$$\frac{1}{\xi}\frac{\mathrm{d}}{\mathrm{d}\xi}\left(\xi\frac{\mathrm{d}\theta_2^s}{\mathrm{d}\xi}\right) = 0, \quad \xi_1 \leqslant \xi \leqslant 1$$

$$\theta_1^s = \theta_2^s \text{ at } \xi = \xi_1; \ \theta_1^s \text{ finite at } \xi = 0$$

$$k_1 \frac{d\theta_1^s}{d\xi} = k_2 \frac{d\theta_2^s}{d\xi} \text{ at } \xi = \xi_1$$

$$\frac{d\theta_2^s}{d\xi} + \gamma\theta_2^s = 0 \text{ at } \xi = 1$$

The solutions are

$$\theta_1^s = A_1 J_0(\beta\xi) - \frac{1}{\alpha}, \quad \beta^2 = \alpha S$$

$$\theta_2^s = A_2 \left[\ln \xi - \frac{1}{\gamma}\right]$$

where

$$A_1 = \frac{1}{\alpha\left[J_0(\beta\xi_1) + \frac{k_1}{k_2}\beta\xi_1 J_1(\beta\xi_1)\left\{\ln \xi_1 - \frac{1}{\gamma}\right\}\right]}$$

$$A_2 = \frac{-\frac{k_1}{k_2}\beta\xi_1 J_1(\beta\xi_1)}{\alpha\left[J_0(\beta\xi_1) + \frac{k_1}{k_2}\beta\xi_1 J_1(\beta\xi_1)\left\{\ln \xi_1 - \frac{1}{\gamma}\right\}\right]}$$

Transient problem

$$\frac{1}{\xi}\frac{\partial}{\partial\xi}\left(\xi\frac{\partial\theta_1^t}{\partial\xi}\right) = \frac{\partial\theta_1^t}{\partial\tau} - \alpha S\theta_1^t, \quad 0 \leqslant \xi \leqslant \xi_1$$

$$\frac{1}{\xi}\frac{\partial}{\partial\xi}\left(\xi\frac{\partial\theta_2^t}{\partial\xi}\right) = \frac{K_1}{K_2}\frac{\partial\theta_2^t}{\partial\tau}, \quad \xi_1 \leqslant \xi \leqslant 1$$

θ_1^t finite at $\xi = 0$

$\theta_1^t = \theta_2^t$ at $\xi = \xi_1, \tau > 0$

$$k_1 \frac{\partial\theta_1^t}{\partial\xi} = k_2 \frac{\partial\theta_2^t}{\partial\xi} \text{ at } \xi = \xi_1, \tau > 0$$

$$\frac{\partial\theta_2^t}{\partial\xi} + \gamma\theta_2^t = 0 \text{ at } \xi = 1, \tau > 0$$

$\theta_1^t = -\theta_1^s$ in $0 \leqslant \xi \leqslant \xi_1, \tau = 0$

$\theta_2^t = -\theta_2^s$ in $\xi_1 \leqslant \xi \leqslant 1, \tau = 0$

This problem is solved by the method of Tittle[6].

We seek a solution of the form

$$\theta_j^{\prime}(\xi, \tau) = \sum_{n=1}^{\infty} A_n X_{jn} e^{-\alpha_j \beta_{jn}^2 \tau} \text{ in region } j;\ j = 1,2.$$

It is easily shown that for region 1 we must have

$$X_{1n}(\xi) = J_0(\lambda_{1n}\xi)$$

where $\lambda_{1n}^2 = \beta^2 + \beta_{1n}^2$ and β_{1n} are the eigenvalues and $\alpha_1 = 1$. Similarly, for region 2 we obtain

$$X_{2n} = B_n [J_0(\beta_{2n}\xi) + C_n Y_0(\beta_{2n}\xi)]$$

and $\alpha_2 = K_2/K_1$.

The eigenvalues β_{2n} are related to β_{1n} by

$$\beta_{1n}^2 = \alpha_2 \beta_{2n}^2$$

The boundary condition at $\xi = 1$ leads to

$$C_n = \frac{\gamma J_0(\beta_{2n}) - \beta_{2n} J_1(\beta_{2n})}{\beta_{2n} Y_1(\beta_{2n}) - \gamma Y_0(\beta_{2n})}$$

Then equating $\theta_1^{\prime}$ and $\theta_2^{\prime}$ at $\xi = \xi_1$ gives

$$B_n = \frac{J_0(\lambda_{1n}\xi_1)}{[J_0(\beta_{2n}\xi_1) + C_n Y_0(\beta_{2n}\xi_1)]}$$

Finally, equating $k_1 \frac{\partial \theta_1^{\prime}}{\partial \xi} = k_2 \frac{\partial \theta_2^{\prime}}{\partial \xi}$ at $\xi = \xi_1$ gives

$$k_1 \lambda_{1n} J_1(\lambda_{1n}\xi_1) = k_2 \beta_{2n} B_n [J_1(\beta_{2n}\xi_1) + C_n Y_1(\beta_{2n}\xi_1)]$$

as the transcendental equation to be solved for the eigenvalues β_{1n} (or β_{2n}).

The coefficients A_n are then given by

$$A_n = \frac{\int_0^{\xi_1} [-\theta_1^{s}] X_{1n}\, \xi d\xi + \left(\frac{K_1}{K_2}\frac{k_2}{k_1}\right) \int_{\xi_1}^{1} [-\theta_2^{s}] X_{2n}\, \xi d\xi}{\int_0^{\xi_1} X_{1n}^2\, \xi d\xi + \left(\frac{K_1}{K_2}\frac{k_2}{k_1}\right) \int_{\xi_1}^{1} X_{2n}^2\, \xi d\xi}$$

The various integrations may be performed giving:

$$\int_0^{\xi_1} [-\theta_1^{s}] X_{1n}\, \xi d\xi = \frac{1}{\alpha}\frac{\xi_1}{\lambda_{1n}} J_1(\lambda_{1n}\xi_1) - \frac{A_1 \xi_1}{\beta_{1n}^2} [\lambda_{1n} J_0(\beta\xi_1) J_1(\lambda_{1n}\xi_1) -$$

$$- \beta J_0(\lambda_{1n}\xi_1) J_1(\beta\xi_1)]$$

$$\int_{\xi_1}^{1} [-\theta_2^{s}] X_{2n}\, \xi d\xi = \frac{A_2 B_n}{\gamma\beta_{2n}} [J_1(\beta_{2n}) - \xi_1 J_1(\beta_{2n}\xi_1) + C_n \{Y_1(\beta_{2n}) -$$

$$- \xi_1 Y_1(\beta_{2n}\xi_1)\}] - \frac{A_2 B_n}{\beta_{2n}} [-\xi_1 \ln \xi_1 J_1(\beta_{2n}\xi_1) + \frac{1}{\beta_{2n}} \{J_0(\beta_{2n}) -$$

$$- J_0(\beta_{2n}\xi_1)\}] - \frac{A_2 B_n C_n}{\beta_{2n}} [-\xi_1 \ln \xi_1 Y_1(\beta_{2n}\xi_1) + \frac{1}{\beta_{2n}} \{Y_0(\beta_{2n}) - Y_0(\beta_{2n}\xi_1)\}]$$

$$\int_0^{\xi_1} X_{1n}^2\,\xi d\xi = \frac{\xi_1^2}{2}\left[J_1^2(\lambda_{1n}\xi_1) + J_0^2(\lambda_{1n}\xi_1)\right]$$

$$\int_{\xi_1}^{1} X_{2n}^2\,\xi d\xi = B_n^2\left[1/2\left\{J_1(\beta_{2n}) + C_n Y_1(\beta_{2n})\right\}^2 + 1/2\left\{J_0(\beta_{2n}) + C_n Y_0(\beta_{2n})\right\}^2 -\right.$$

$$\left. - \frac{\xi_1^2}{2}\left\{J_1(\beta_{2n}\xi_1) + C_n Y_1(\beta_{2n}\xi_1)\right\}^2 - \frac{\xi_1^2}{2}\left\{J_0(\beta_{2n}\xi_1) + C_n Y_0(\beta_{2n}\xi_1)\right\}^2\right]$$

RESULTS AND DISCUSSION

Numerical calculations were performed on the CDC-6400 computer at the University of Arizona Computer Center. Figs. 1–3 show centerline transient temperature response for various heating rates for three different values of the wall-thickness parameter ξ_1. In each case, the dimensionless heat-transfer coefficient, γ, is equal to infinity (corresponding to a constant outer wall temperature). Table I lists the values of the properties used in making these calculations. For a cooling-bath temperature of 0°C and a maximum allowable temperature in the column of 37°C, we find the maximum allowable value of θ to be 0.1355. This maximum allowable value of θ is denoted θ_c.

An inspection of Figs. 1–3 shows that for a given value of ξ_1, there will be some value of S below which θ_c will never be exceeded and above which θ_c will always be

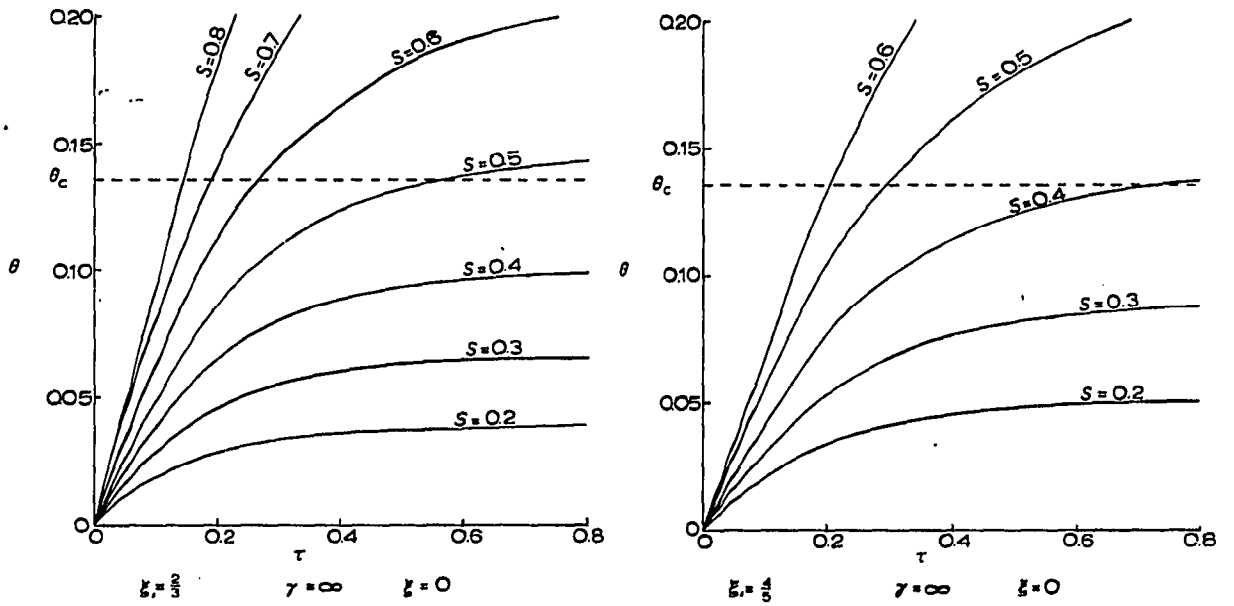

Fig. 1. Centerline transient temperature response for $\xi_1 = 2/3$, $\gamma = \infty$.

Fig. 2. Centerline transient temperature response for $\xi_1 = 4/5$, $\gamma = \infty$.

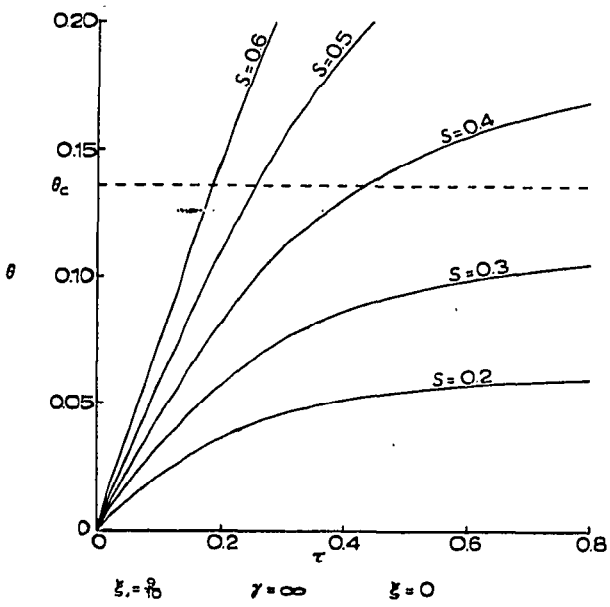

Fig. 3. Centerline transient temperature response for $\xi_1 = 9/10$, $\gamma = \infty$.

exceeded in some finite amount of time. We term this value of S for which θ_c is approached asymptotically $S_{max.}$, and its variation with ξ_1 is shown in Fig. 4.

For the sake of comparison, Fig. 5 shows centerline transient temperature response for a value of the dimensionless heat-transfer coefficient equal to unity. It is clear from this figure that effective cooling is extremely important if one is to use high enough electric field strengths to give acceptable resolution while refraining from "cooking" the sample.

Because the electric field decreases in going from terminator to leader electrolyte zones, S will also decrease from terminator to leader. Fig. 6 depicts the steady-state temperature profile for various values of S. Because ionic mobility is proportional to temperature, this leads to velocity profiles that become progressively less "bowed" from terminator to leader zones.

Fig. 7 shows steady-state temperature distributions for various values of ξ_1 with the heating rate in each case equal to $S_{max.}$. This figure demonstrates the advantage of thick-walled columns as the total temperature drop within the column

TABLE I

DATA USED FOR CALCULATIONS

Parameter	*Value*
k_1	$13.9 \cdot 10^{-4}$ cal·cm^{-1}·sec^{-1}·°K^{-1}
k_2	$26.7 \cdot 10^{-4}$ cal·cm^{-1}·sec^{-1}·°K^{-1}
K_1	$14.779 \cdot 10^{-4}$ cm^2/sec
K_2	$59.333 \cdot 10^{-4}$ cm^2/sec
α	7.75

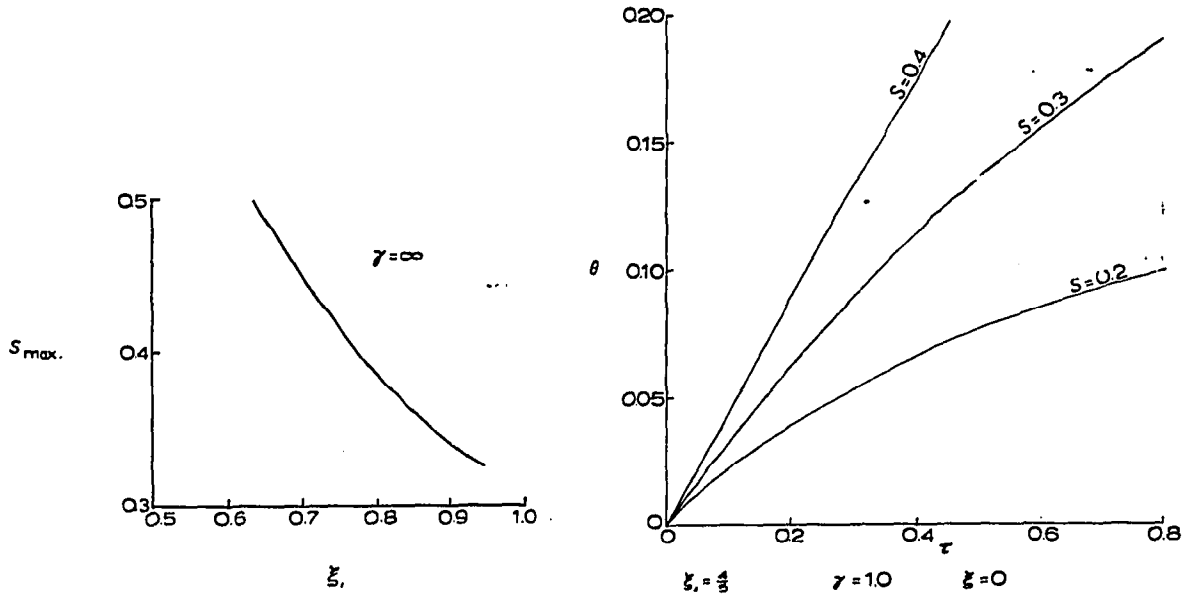

Fig. 4. Variation of maximum heating rate with wall-thickness parameter, $\gamma = \infty$.

Fig. 5. Centerline transient temperature response for $\xi_1 = 4/5$, $\gamma = 1$.

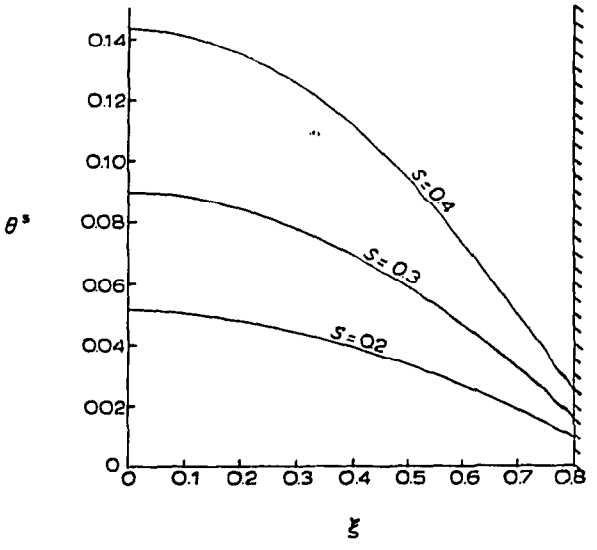

Fig. 6. Steady-state temperature profiles based on a linear variation of electrical conductivity with temperature, $\xi_1 = 0.8$, $\gamma = \infty$.

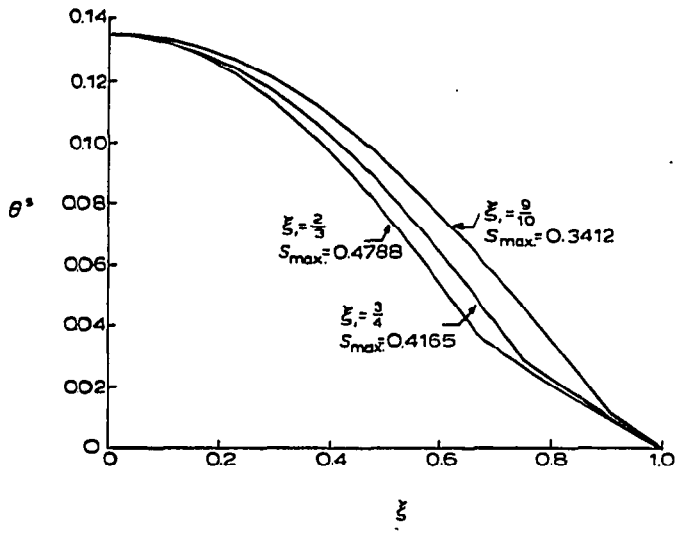

Fig. 7. Steady-state temperature profiles for $S = S_{max.}$.

(and hence velocity variation or "bowing" effect) is seen to increase considerably with decreasing wall thickness.

It is interesting to compare the present analysis with the parabolic temperature distributions predicted by previous investigators. The results of Konstantinov and Oshurkova[2] may be written, in terms of our nomenclature, as

$$\theta^s = \frac{S}{4}\left(1 - \frac{\xi^2}{\xi_1^2}\right) \qquad 0 \leqslant \xi \leqslant \xi_1.$$

The above equation is shown plotted in Fig. 8. Comparison with Fig. 6 shows that the parabolic distribution tends to underpredict the temperature, the discrepancy increasing with increasing heating rate. At a value of S equal to 0.4, Fig. 8 predicts that the maximum value of θ will be 26.2% less than θ_c. From Fig. 6, however, it is seen that at $S = 0.4$, the maximum value of θ is actually 6% greater than θ_c. Thus a design based on a parabolic temperature distribution could lead one to believe that a large margin of safety exists with respect to preserving living cells, whereas the actual temperature rise would surely be destructive to such cells.

Because the sharpness of ionic interfaces increases with increasing electric field strength[7], it may be desirable to operate at values of S greater than $S_{max.}$. This requires that E and R_1 be chosen in such a way that the time required for separation be less than the time at which θ_c is exceeded. Brouwer and Postema[8] have presented an approximate equation for determining the time required for separation. Assuming their optimal condition (conductivity of the terminating zone approaching that of the sample solution) and using a mobility difference of $2 \cdot 10^{-4}$ cm$^2 \cdot$V$^{-1} \cdot$sec^{-1}, an adapted sample length of 1 cm, and the data of Table I, their result may be written as

$$\tau_s = 0.0052965 \frac{E}{S}.$$

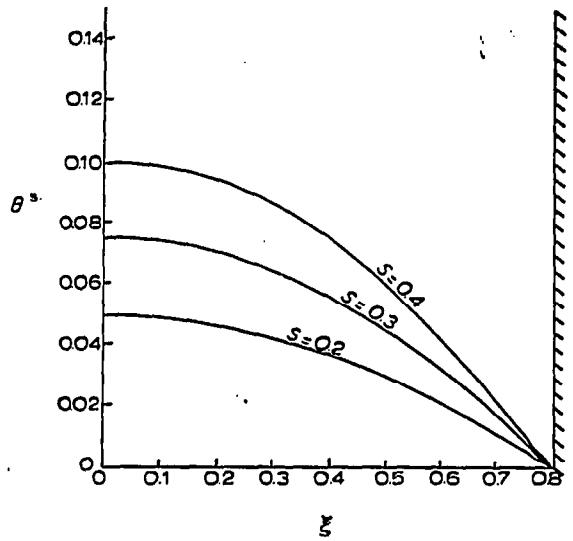

Fig. 8. Steady-state temperature profiles based on constant electrical conductivity (plotted from results given in ref. 2). Comparison with Fig. 6 shows the degree to which results based on constant electrical conductivity underpredict the actual temperature distribution. $\xi_1 = 0.8$, $\gamma = \infty$

From plots such as those in Figs. 1–3, one can determine for a given ξ_1 the variation of τ_c with S. Then, if one stipulates a value for the ratio τ_s/τ_c (thus assuring $\tau_s < \tau_c$), one may determine the variation of τ_s with S. Using this and the above equation, one can determine how E varies with S. Finally, using the definition of S one can determine the corresponding values of R_2, and hence also R_1, for the given ξ_1. Fig. 9

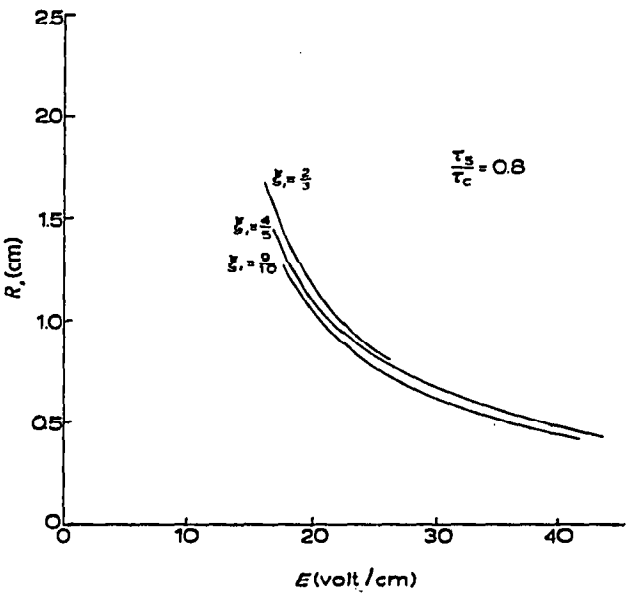

Fig. 9. Variation of internal column radius with electric field for $\tau_s/\tau_c = 0.8$. This figure clearly demonstrates the advantages of thick-walled columns.

shows the variation of R_1 with E for various values of ξ_1 for a value of τ_s/τ_c of 0.8. Again the advantage of thick-walled columns can be seen. For a given internal wall radius, the use of thicker-walled columns allows larger values of electric field strength to be used, thus increasing resolution. On the other hand, for a given value of electric field strength, thicker-walled columns allow the use of larger internal radii. This fact is particularly important for preparative electrophoresis.

CONCLUSION

The present analysis, based on a linear variation of electrical conductivity with temperature and taking into account the effects of a finite wall thickness, is seen to be a major improvement over previous analyses, which predict parabolic temperature distributions. Previous analyses are seen to underpredict considerably the actual temperature variation in the isotachophoretic column, leading to the possibility of designs allowing temperature rises hazardous to living cells. It was shown that for higher resolution, operation at values of S greater than $S_{max.}$ might be desirable, thus necessitating the solution to the transient problem presented here. It was also shown to be advantageous to use thick-walled columns both from the point of view of higher resolution and of increased production.

ACKNOWLEDGEMENTS

The authors wish to express their gratitude to Dr. Milan Bier and J. O. N. Hinckley for their interest and comments in discussion. Thanks are also due to Dr. R. E. Petersen for verifying the calculations made here.

This study was funded by the National Aeronautics and Space Administration under Contract NAS8-29566.

APPENDIX

COMPARISON OF "EXACT" SOLUTION OF STEADY-STATE TEMPERATURE DISTRIBUTION ASSUMING CONSTANT THERMAL PROPERTIES WITH A STEADY-STATE PERTURBATION SOLUTION PERMITTING LINEAR TEMPERATURE DEPENDENCE OF THERMAL PROPERTIES

(1) The constant-properties solution

The solution of the steady-state problem assuming constant thermal properties (density, specific heat, and thermal conductivity) has been given. For the special case where $T_2 = T_\infty$ at $r = R_2$ we have:

$$\theta_1^s = \frac{J_0(\beta\xi)}{\alpha\left[J_0(\beta\xi_1) + \frac{k_1}{k_2}\beta\xi_1 J_1(\beta\xi_1)\ln\xi_1\right]} - \frac{1}{\alpha}$$

from which the maximum temperature, at $\xi = 0$, is

$$\theta_{1\,max.}^s = \frac{1}{\alpha}\left\{\frac{1}{\left[J_0(\beta\xi_1) + \frac{k_1}{k_2}\beta\xi_1 J_1(\beta\xi_1)\ln\xi_1\right]} - 1\right\}$$

For the purposes of obtaining a numerical comparison with the perturbation solution given below we have chosen the following values for the parameters involved: $\xi_1 = 2/3$; $\alpha = 7.75$; $\theta^s_{1_{max.}} = 0.1355$; $k_1 = 13.9 \cdot 10^{-4}$ cal·cm^{-1}·sec^{-1}·°K^{-1}; $k_2 = 26.7 \cdot 10^{-4}$ cal·cm^{-1}·sec^{-1}·°K^{-1}.

The values of k_1 and k_2 are average values for the range of θ^s considered, *i.e.* $0 \leqslant \theta^s \leqslant \theta^s_{1_{max.}}$.

Solving for $\beta = \sqrt{\alpha S}$ then gives a value for the maximum permissible value of the dimensionless heat source strength S.

We find that $S_{max.} = 0.480$.

(2) Perturbation solution for the steady-state problem

The statement of the problem in terms of the dimensionless variables is:

$$\frac{1}{\xi}\frac{\mathrm{d}}{\mathrm{d}\xi}\left[\xi\,(1 + \beta_1\,\theta^s_1)\,\frac{\mathrm{d}\theta^s_1}{\mathrm{d}\xi}\right] = -S\,(1 + \alpha\theta^s_1), \quad 0 \leqslant \xi \leqslant \xi_1$$

$$\frac{1}{\xi}\frac{\mathrm{d}}{\mathrm{d}\xi}\left[\xi\,(1 + \beta_2\,\theta^s_2)\,\frac{\mathrm{d}\theta^s_2}{\mathrm{d}\xi}\right] = 0, \quad \xi_1 \leqslant \xi \leqslant 1$$

where now

$$k_1 = k_{10}\,(1 + \beta_1\,\theta^s_1)$$

$$k_2 = k_{20}\,(1 + \beta_2\,\theta^s_2)$$

and k_{10}, k_{20} are the values of k_1, k_2 at $\theta^s_{1,2} = 0$.
Boundary conditions are taken to be

$$\theta^s_2 = 0 \text{ at } \xi = 1$$

$$\theta^s_1 = \theta^s_2 \text{ at } \xi = \xi_1$$

$$k_1\frac{\mathrm{d}\theta^s_1}{\mathrm{d}\xi} = k_2\frac{\mathrm{d}\theta^s_2}{\mathrm{d}\xi} \text{ at } \xi = \xi_1$$

and the temperature at $\xi = 0$ must be finite.

We proceed by assuming that θ can be expanded in terms of a power series in the dimensionless source strength S.

$$\theta^s_1(\xi; S) \sim S\mathrm{f}_0(\xi) + S^2\,\mathrm{f}_1(\xi) + S^3\,\mathrm{f}_2(\xi) + \ldots, \quad 0 \leqslant \xi \leqslant \xi_1$$

$$\theta^s_2(\xi; S) \sim S\varphi_0(\xi) + S^2\,\varphi_1(\xi) + S^3\,\varphi_2(\xi) + \ldots, \quad \xi_1 \leqslant \xi \leqslant 1.$$

The obvious procedural steps are not reproduced here; instead we shall quote the solution of θ^s_1 which we require for comparative purposes.

We obtain the following:

$$\theta^s_1 = S\left[B_1 - \frac{\xi^2}{4}\right] + S^2\left[(\beta_1 - \alpha)\left(\frac{B_1\,\xi^2}{4} - \frac{\xi^4}{64}\right) - \frac{\beta_1\,\xi^4}{64} + D_1\right] + \ldots,$$

$$0 \leqslant \xi \leqslant \xi_1$$

where

$$B_1 = \frac{\xi_1^2}{4} - \frac{k_{10}}{k_{20}} \frac{\xi_1^2}{2} \ln \xi_1$$

$$D_1 = C \ln \xi_1 - \frac{\beta_2 A^2}{2} (\ln \xi_1)^2 - (\beta_1 - \alpha) \left(\frac{B_1 \xi_1^2}{4} - \frac{\xi_1^4}{64} \right) + \frac{\beta_1 \xi_1^4}{64}$$

$$C = \frac{k_{10}}{k_{20}} \left[(\beta_1 - \alpha) \left(\frac{B_1 \xi_1^2}{2} - \frac{\xi_1^4}{16} \right) - \frac{\beta_1 \xi_1^4}{16} - \beta_1 \left(\frac{B_1 \xi_1^2}{2} - \frac{\xi_1^4}{8} \right) \right]$$

$$A = -\frac{k_{10}}{k_{20}} \frac{\xi_1^2}{2}$$

For $\theta^s_{1_{max.}}$ at $\xi = 0$ we then have simply

$$\therefore \theta^s_{1_{max.}} = SB_1 + S^2 D_1 + \ldots$$

Numerical calculations assume the same values used in section 1 except that we now use: $k_{20} = 26 \cdot 10^{-4}$ cal·cm^{-1}·sec^{-1}·°K^{-1}; $k_{10} = 13.19 \cdot 10^{-4}$ cal·cm^{-1}·sec^{-1}·°K^{-1}; $\beta_2 = 0.42$; $\beta_1 = 0.808$.
We now find a value for $S_{max.}$.

$$S_{max.} = 0.576 \text{ (variable properties).}$$

This value may be compared directly with that obtained from the perturbation scheme by setting $\beta_1 = \beta_2 = 0$ and replacing k_{10}, k_{20} by the average values for k_1, k_2 used in section 1, in which case we get

$$S_{max.} = 0.561 \text{ (constant properties).}$$

Thus we see that within the perturbation steady state solution, taken to two terms, the effect of neglecting thermal property variations leads to a difference of some 2.5% in the calculation of $S_{max.}$. Furthermore we note that the result obtained by assuming constant properties is conservative.

(3) Comparison with the "exact" solution

It will be noted that the value of $S_{max.} = 0.48$ given in section 1 is some 14.5% below that obtained from the two-term perturbation method also assuming constant properties. This, however, is a result of relatively slow convergence of the perturbation expansion. We have continued the expansion to three terms (assuming constant properties) and then obtain $S_{max.} = 0.51$, which is only 6% higher than the "exact" solution. We conclude therefore that the error in neglecting the thermal properties dependence on temperature is justified and is probably less than 3% in view of the comparisons made within the perturbation solutions. Moreover, the "exact" constant-properties solution gives a conservative answer and is therefore safe for design calculations.

LIST OF SYMBOLS

Symbol	*Meaning*	*Unit*
c	Specific heat	$cal \cdot g^{-1} \cdot {}^{\circ}K^{-1}$
E	Electric field	V/cm
h	Heat-transfer coeefficient	$cal \cdot cm^{-2} \cdot sec^{-1} \cdot {}^{\circ}K^{-1}$
J	Mechanical equivalent of heat	cal/J
J_0	Bessel function of the first kind of order zero	
J_1	Bessel function of the first kind of order one	
K	Thermal diffusivity	cm^2/sec
k	Thermal conductivity	$cal \cdot cm^{-1} \cdot sec^{-1} \cdot {}^{\circ}K^{-1}$
Q_e	Heat generation per unit volume	$cal \cdot cm^{-3} \cdot sec^{-1}$
r	Radial distance	cm
R_1	Internal radius of column	cm
R_2	External radius of column	cm
S	Dimensionless heating rate	
T	Temperature	°K
t	Time	sec
Y_0	Bessel function of the second kind of order zero	
Y_1	Bessel function of the second kind of order one	
α	Dimensionless coefficient of electrical conductivity	
γ	Dimensionless heat-transfer coefficient	
θ	Dimensionless temperature	
ξ	Dimensionless radial distance	
ξ_1	Dimensionless wall-thickness parameter	
ϱ	Mass density	g/cm^3
σ	Electrical conductivity	$\Omega^{-1} \cdot cm^{-1}$
τ	Dimensionless time	
τ_c	Dimensionless time required to reach θ_c	
τ_s	Dimensionless time required for separation	

Subscripts

1	Refers to properties of the electrolyte solution.
2	Refers to properties of the column wall.
∞	Refers to properties of the cooling bath surrounding the isotachophoresis column.

Superscripts

s	Refers to steady-state conditions.
t	Refers to transient conditions.

REFERENCES

1 A. J. P. Martin and F. M. Everaerts, *Proc. Roy. Soc., London, Sect. A.*, 316 (1970) 493.
2 B. P. Konstantinov and O. V. Oshurkova, *Sov. Phys. Tech. Phys.*, 11 (1966) 693.
3 S. Hjertén, *Chromatogr. Rev.*, 9 (1967) 122.
4 R. J. Routs, *Electrolyte Systems in Isotachophoresis and Their Application to Some Protein Separations*, Solna Skriv- & Stenograftjanst AB, Solna, 1971, p. 41.
5 J. F. Brown and J. O. N. Hinckley, personal communication.
6 C. W. Tittle, *J. Appl. Phys.*, 36 (1965) 1486.
7 M. Coxon and M. J. Binder, *J. Chromatogr.*, 95 (1974) 133.
8 G. Brouwer and G. A. Postema, *J. Electrochem. Soc.*, 117 (1970) 874.